

Effects of cholesterol on the mechanism of fengycin, a biofungicide

Sreyoshi Sur¹ and Alan Grossfield^{2,*}

¹Department of Chemistry, University of Rochester, Rochester, NY and ²Department of Biochemistry and Biophysics, University of Rochester Medical Center, Rochester, NY

ABSTRACT Fengycins are a class of antifungal lipopeptides synthesized by the bacteria *Bacillus subtilis*, commercially available as the primary component of the agricultural fungicide Serenade. They are toxic to fungi but far less to mammalian cells. One key difference between mammalian and fungal cell membranes is the presence of cholesterol only in the former; recent experimental work showed that the presence of cholesterol reduces fengycin-induced membrane leakage. Since our previous all-atom and coarse-grained simulations suggested that aggregation of membrane-bound fengycin is central to its ability to disrupt membranes, we hypothesized that cholesterol might reduce fengycin aggregation. Here, we test this hypothesis using coarse-grained molecular dynamics simulations, with sampling enhanced via the weighted ensemble method. The results indicate that cholesterol subtly alters the size distribution for fengycin aggregates, limits the lateral range of their membrane disordering, and reduces the ability of aggregates to bend the membrane. Taken together, these phenomena may account for cholesterol's effects on fengycin activity.

SIGNIFICANCE Fengycins are cyclic lipopeptides, used agriculturally as biofungicides. They specifically disrupt the fungal cell membrane and have significantly reduced effects on mammals and other animals. Fengycins have also been studied as a potential antifungal treatment. For this reason, it is important to understand why fengycins affect fungal cell membranes more than mammalian membranes. We used an enhanced sampling technique called the weighted ensemble method along with molecular dynamics simulations to understand the effects of fengycins on model membranes with and without cholesterol, testing the primary difference between mammalian and fungal membranes. The results indicate that cholesterol alters the effects of fengycins on membrane structure and dynamics.

INTRODUCTION

The world human population has reached 7.8 billion as of August 2021 (1), which creates ever greater pressure to increase agricultural yields (2). Every year, crops are destroyed by various microbial infections, of which 60% are caused by fungus (3). Various antibiotics have been synthesized, like amphotericin B, natamycin, and nystatin, to treat infections in humans, but fungi and bacteria are developing resistance to these compounds (4–6).

With this in mind, many groups are interested in developing new ecofriendly antifungals suitable for agricultural usage (7). Fengycins are a class of lipopeptides synthesized by the bacteria *Bacillus subtilis*, which specifically kills certain fungal species (8,9). Fengycins, along with surfac-

tins and iturins, are the primary active components of Serenade (Bayer), a commercial fungicide and bactericide, which is used to treat plant diseases, like clubroot disease (*Plasmodiophora moniliforme*), barley head blight (*Fusarium graminearum*), cucurbit powdery (*Podosphaera fusca*), black Sigatoka (*Mycosphaerella fijiensis*), gray mold (*Botrytis cinerea*), and soft rot (*Rhizopus stolonifer*) (10–19).

The effects of fengycin seem specific to fungal cells, with far less effect on animals. This is part of its “green” signature, since neither the agricultural workers applying it nor the animals in the surrounding environment are adversely affected by its application. It would be advantageous to understand why this is the case, particularly given that it has drawn medical interest as a potential antifungal skin ointment (20–22).

Previous calorimetric studies suggested that fengycins cause order to disorder phase transitions and partition into the cholesterol-rich phase in the stratum corneum

Submitted August 2, 2021, and accepted for publication April 5, 2022.

*Correspondence: alan_grossfield@urmc.rochester.edu

Editor: Heiko Heerklotz

<https://doi.org/10.1016/j.bpj.2022.04.006>

© 2022 Biophysical Society.

Sur and Grossfield

(outermost skin layer) model and in monolayers mimicking them (23,24). This implies that either fengycin prefers a more lipid disordered phase or that it preferentially interacts with cholesterol.

To better understand the mechanism of fengycin's selectivity, Heerklotz and coworkers conducted fluorescence lifetime experiments with model membranes of varying phospholipid and sterol composition (25,26). They showed that higher concentrations of fengycin were required to induce leakage when the vesicles contain cholesterol, indicating that cholesterol inhibits fengycin. The authors discussed two possible mechanisms for this phenomenon: 1) graded leakage, where the fengycins induce general overall leakiness by thinning the membrane and disordering the lipid acyl chains, or 2) all-or-none leakage, where long-lived pores form that cause the vesicles to drain quickly and completely (27). Patel et al. (27) showed that fengycin follows an all-or-none mechanism using these methods, although Fiedler and Heerklotz (28) found that the tolerable fraction of fengycins on the membrane surface increases in a mixture of palmitoyl-oleoyl-phosphatidyl choline (POPC) and cholesterol membranes compared with pure POPC. The purported presence of pores suggests that fengycin must aggregate on the membrane surface to function, and although no experiments have been able to demonstrate this effect directly, Fiedler and Heerklotz (28) hypothesized that fengycins preferentially interact with cholesterol and thus are unable to aggregate, reducing membrane permeabilization.

Thus, we hypothesize that fengycins fail to induce leakage in lipid vesicles containing cholesterol for one or more of the following reasons: 1) cholesterol inhibits fengycin aggregation by improving miscibility of fengycins with other lipids or preferentially interacting with fengycins; 2) cholesterol changes fengycin's propensity to aggregate or reduces the size of those aggregates, rendering them inactive; and 3) cholesterol does not affect the fengycin aggregates but increases membrane order and renders the membrane resistant to thinning and leakage. Molecular dynamics simulations are an excellent tool to fill in this missing connection, since their molecule-scale resolution neatly matches the problem. However, obtaining sufficient sampling still remains an issue; lateral reorganization of the membrane and protein conformational change are both slow processes compared with the timescale of most molecular dynamics simulations. Use of coarse-grained simulations reduces the computational cost of sampling, as does our application of the weighted ensemble method (29,30).

Previous work from our group showed that fengycin aggregation was higher in a zwitterionic lipid membrane chosen to model eukaryotes, compared with anionic membranes chosen to mimic bacteria, and that aggregation was crucial to disordering the membrane (31,32). Here, we study a more subtle variation, the effect of cholesterol on fengycin aggregation in the backdrop of a simple zwitterionic bilayer.

MATERIALS AND METHODS

System construction

All the particles in our systems were modeled using the MARTINI coarse-grained force field v.2.2P (33). We considered two lipid compositions: pure POPC and a 4:1 mixture of POPC and cholesterol. The POPC systems contained 186 POPC molecules per leaflet, with 8,352 waters, and 99 Na⁺ and 84 Cl⁻ ions. Each composition was run with 15 fengycin molecules added to the upper leaflet; neat lipid simulations were run for comparison purposes. The systems containing fengycin contained an additional 15 sodium ions to maintain electroneutrality. The parameters for fengycin were adapted from Horn et al. (31), after accounting for force field updates. For lipids, we used MARTINI v.2.0, whereas the peptide part of fengycin was modeled with MARTINI v.2.2 (29,33,34). In addition, we used the MARTINI parameters for cholesterol v.2.0 with virtual sites (35). All the parameters are available in our github repository mentioned at the end of this section. The chemical structure of fengycin is shown in Fig. 1 A; this variant is also referred to as plipastatin A in the literature. The sequence differs slightly from the one we simulated previously, with glutamate replaced with glutamine in the position 7 as shown in Fig. 1 A (31).

Initially, we randomly placed fengycins in a plane parallel to the bilayer, with each fengycin 20 Å above the bilayer center and the acyl chain pointing toward the membrane center. We constructed the rest of the membrane around them using INSANE (36) and added NaCl for an effective salt concentration of 150 mM using GROMACS genion tool. (37). The final box size was 107 × 107 × 135 Å. Next, we relaxed each system with 10,000 steps of energy minimization, followed by 10–15 ns of molecular dynamics simulations with a time step of 2 fs. All calculations were performed using GROMACS v.2016.3 (37). The Table 1 shows all the details about the systems we built.

Simulation details

We used the GROMACS v.2016.3 to perform the molecular dynamics simulations (37). We used a time step of 20 fs, updating the nearest neighbor list every 20 steps. The simulations were run in an isobaric-isothermal ensemble with the Parrinello-Rahman barostat (38) and the velocity rescaling thermostat (39). The temperature and pressure were kept at 310 K and 1 atm, respectively. Electrostatic interactions were calculated using the reaction field method (40). The Verlet scheme was used to compute the van der Waals forces using an 11-Å cutoff. The cumulative time of the simulation is shown in Table 1.

Weighted ensemble method

We used the weighted ensemble method to calculate the probability distribution for fengycin aggregation (30), implemented via the WESTPA software package (41,42). In this method, no additional bias or force is added to the system to enhance the sampling. Rather, structures are binned along a predetermined progress coordinate, and trajectories are split and merged to maintain a target number of trajectories in each populated bin, with the overall statistical weight tracked appropriately.

We quantify the aggregation of fengycin by using as progress coordinate the total number of contacts between fengycin molecules. The contact value for a pair of fengycins i and j is

$$S_{ij} = \frac{1}{1 + \left(\frac{r_{ij}}{r_0}\right)^6}, \quad (1)$$

where r_{ij} is the lateral distance between the centroids of the peptide part of fengycins and $r_0 = 10$ Å. The total number of contacts for a given frame in the trajectory is the sum of S_{ij} between all pairs of fengycins,

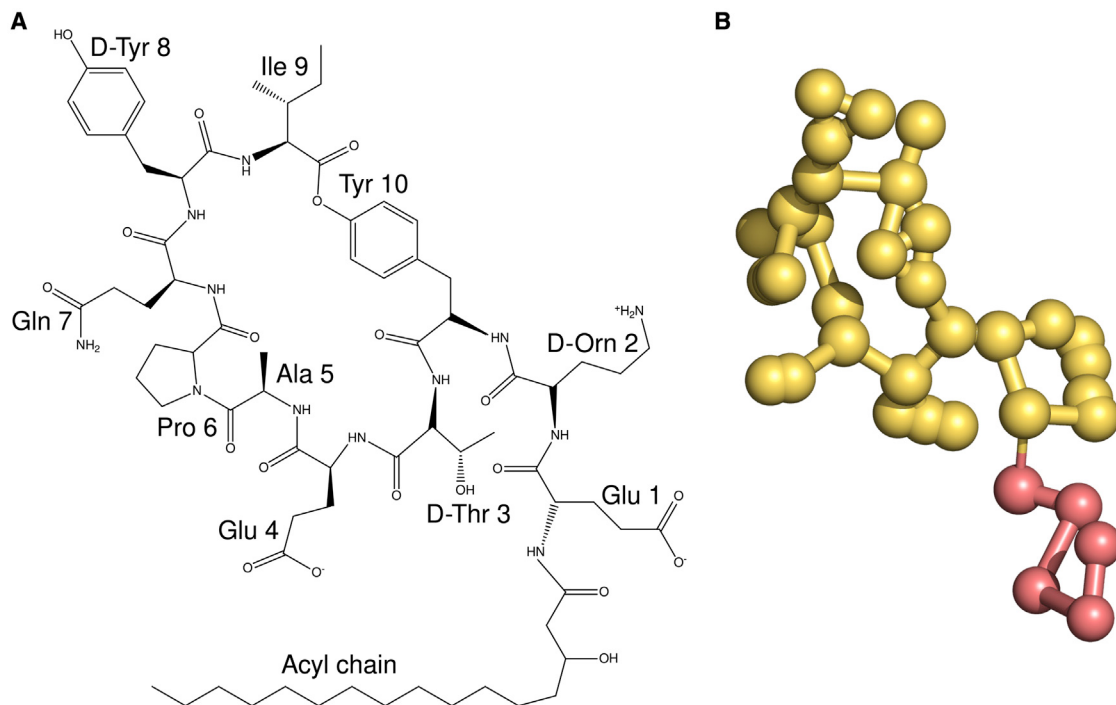


FIGURE 1 (A) Chemical structure of fengycin. (B) Coarse-grained model of fengycin. To see this figure in color, go online.

$$C_{ij} = \sum_{i \neq j} S_{ij}. \quad (2)$$

$$S_{mol} = \left| \left\langle \frac{3\cos^2\theta - 1}{2} \right\rangle \right|, \quad (3)$$

This progress coordinate was divided into 25 evenly spaced bins, each bin having a width of 1.0.

Each iteration of weighted ensemble simulations involves two stages. First, each starting structure is subjected to 5 ns of molecular dynamics simulations. At the end of the dynamics, each trajectory is assigned to a bin based on its total contact value (C_{ij} from Eq. 2). We chose to target five trajectories to each populated bin. If there were more than five in a given bin, pairwise approach is used to prune a trajectory. Within the five trajectories, two are chosen at random, of which only one with relatively less weight is pruned and the weight of the pruned trajectory is assigned to the surviving trajectory. If there were fewer than five trajectories, a trajectory was chosen at random and split, with its weight equally shared with the resulting children. The total weight of all the trajectories for a particular iteration should always be 1.0 (30,41).

Simulation analysis

Lightweight object-oriented structure analysis library (LOOS) was used to analyze all the data, along with the analysis tools that came with the WESTPA software (41,43–45). All the analysis was performed at 1-ns resolution. All average quantities were computed using the last 50 weighted ensemble (WE) iterations, taking into account the weight associated with each trajectory. Unless otherwise specified, error bars are the standard errors calculated by treating each WE simulation as one independent measurement.

Molecular order parameters

The molecular order parameter is a whole-chain analog of the deuterium order parameters measured using solid-state nuclear magnetic resonance (46). It is calculated as

where θ is the angle between the membrane normal (z axis) and the second and third principal axes of the acyl chain; this method is implemented in the *dibmops* tool in LOOS.

Area per lipid

The area per lipid is computed by calculating the area occupied by the membrane using the periodic box dimensions for each frame of a trajectory and then dividing the area by the number of lipids and sterols present in each leaflet. We used the *area_per_lipid* command line tool implemented in LOOS to do this calculation.

Radial distribution function

We used the LOOS tool *xy_rdf* to calculate the two-dimensional lateral radial distribution function in the plane of the membrane for various membrane components (lipid, cholesterol, and fengycin); this tool operates on the molecules' centroid rather than any individual atoms.

TABLE 1 Summary of simulations

Membrane	Peptides	Length (μs)	Replicates	Method
PC	15	~ 350	3	WE
PC:CHOL	15	~ 330	3	WE
PC	0	~ 0.6	3	MD
PC:CHOL	0	~ 0.6	3	MD

For the WE runs, the time refers to the total sampling time for each WE replicate. “Replicates” indicate the number of independently built trajectories that were run; three distinct WE simulations were performed for each composition. MD, standard molecular dynamics; WE, weighted ensemble.

Sur and Grossfield

Probability distribution for fengycin-fengycin contacts and fengycin-lipid contacts

We used the tool *w_pdist* from WESTPA to compare weighted population distributions along the progress coordinate for each WE iteration. *plotlist* (also part of WESTPA) was used to plot time series of this distribution, as well as averages over specific ranges of iterations.

Aggregation propensity

When quantifying aggregation, we considered two fengycins to be in contact if they had 50 pairs of atoms less than 6.5 Å apart; these specific values were chosen to reproduce manual assignments made by eye in a subset of trial frames. Using this criterion, we tracked the size distribution of fengycin aggregates through the WE runs. As above, we used *w_pdist* and *plotlist* to create weighted histograms for the number of fengycin-fengycin contacts and the total number of aggregates (41,42).

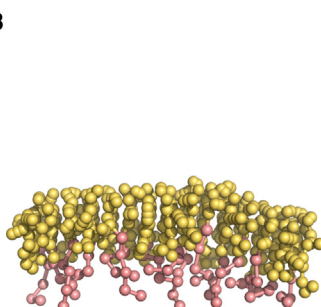
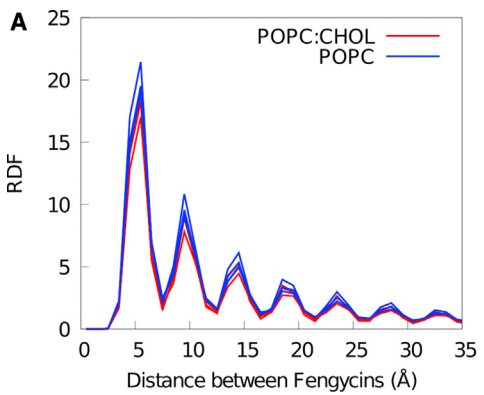
Z position of phosphate heads

We tracked the deformation of the membrane by calculating the z position of the phosphate bead of each POPC with respect to the center of membrane. These distances were binned with respect to the lateral distance to the nearest fengycin's centroid. To simplify comparison between systems with and without cholesterol, we subtracted the thickness of the corresponding pure membranes to measure the perturbation caused due to fengycin.

All the analysis scripts and the MARTINI parameter files are available as a github repository at <https://github.com/sreyoshi09/scripts.git>.

RESULTS

Our previous work showed that larger aggregates survive for a longer lifetime in POPC bilayers compared with POPE:POPG ones (32). Previous experimental work indicated that cholesterol reduces the ability of fengycin to induce membrane leakage and hypothesized the presence of specific cholesterol-fengycin interactions to account for it (28). We test this hypothesis using our molecular dynamics simulations. We also test two alternative hypotheses: 1) does cholesterol change the aggregation propensity of fengycin, such that it is less able to induce membrane deformation and leakage, and 2) does cholesterol render the membrane resistant to fengycin aggregates?



Fengycin forms ordered aggregates

Fig. 2 A shows the lateral radial distribution function for fengycin molecules. The large first peak indicates a strong tendency to oligomerize, although numerous secondary peaks indicate the presence of higher order structures. It seems that fengycin has a tendency to form some solid-gel systems as evident from their solid-like radial distribution function. Furthermore, the fact that the peaks are equally spaced, well resolved, and of similar width strongly suggests that the aggregates are linear, a fact we verified visually (see **Fig. 2 B**). Although previous coarse-grained simulations also showed the presence of linear aggregates, our more recent all-atom simulations suggest the aggregates were more amorphous, consistent with atomic force microscopy experiments from Eeman et al. (31,32,22). It is worth noting that the MARTINI coarse-grained model is known to overestimate the aggregation propensity of membrane proteins (47).

Aggregation propensity similar with or without cholesterol

Fiedler and Heerklotz's (28) fluorescence lifetime experiments suggested that cholesterol reduces fengycin-induced membrane leakage by reducing fengycin's ability to aggregate in the membrane. One of the primary goals of the present work is to test this hypothesis. In this section, we use the probability distribution of fengycin-fengycin contacts as a measure of their propensity to aggregate.

As discussed in the section [probability distribution for fengycin-fengycin contacts and fengycin-lipid contacts](#), we track aggregation by counting the number of fengycin-fengycin contacts; the resulting probability distribution is shown as **Fig. 3**. Somewhat surprisingly, the data indicate that the presence of cholesterol slightly increases the tendency of fengycin to aggregate. Although the peak of the probability distribution is virtually identical, the tail to lower numbers of contacts is wider in the membrane without cholesterol, which also contains a measurable population of fully dispersed fengycin molecules.

FIGURE 2 (A) Lateral radial distribution function (RDF) between fengycins. Each curve represents the average from a single weighted ensemble run. (B) Structure of a single 15-mer aggregate. To see this figure in color, go online.

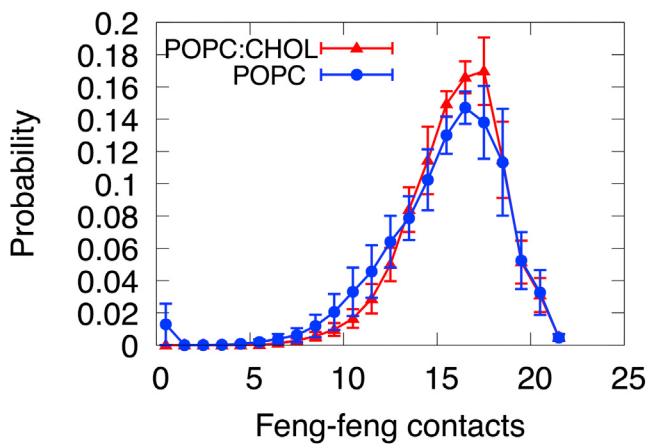


FIGURE 3 Probability distribution for fengycin-fengycin contacts. The number of fengycin contacts is calculated using Eqs. 1 and 2. Error bars are the standard error, calculated by considering each weighted ensemble run as a single independent measurement. To see this figure in color, go online.

Reducing the complex phenomenon of aggregation to a single progress coordinate necessarily reduces the amount of information available. To recover some of this informa-

tion, we also track a two-dimensional probability distribution, as a function of number of contacts and the number of distinct aggregates, which allows us to distinguish potential changes in the morphology of the clusters.

The results are shown in Fig. 4. Fig. 4, A and B shows the distributions in the POPC and POPC:cholesterol membranes, respectively. Since the two distributions are fairly similar, we show the difference between them as Fig. 4C. Focusing on Fig. 4C, it is clear that the fengycins are more likely to be found as a single large aggregate in the presence of cholesterol, whereas in a pure POPC membrane, there is more diversity in both the number of contacts and number of distinct aggregates.

Fig. 4, D–F indicates the kinds of aggregation consistent with specific parts of the probability distribution. Most notably, Fig. 4E shows that, when we have relatively high numbers of contacts and numbers of aggregates, this generally indicates the presence of one or two major aggregates, plus a number of isolated monomers.

The above sections demonstrate that there is only a subtle alteration in favorable fengycin-fengycin interaction in the presence or absence of cholesterol, but the shape and morphology of those aggregates is somewhat sensitive to

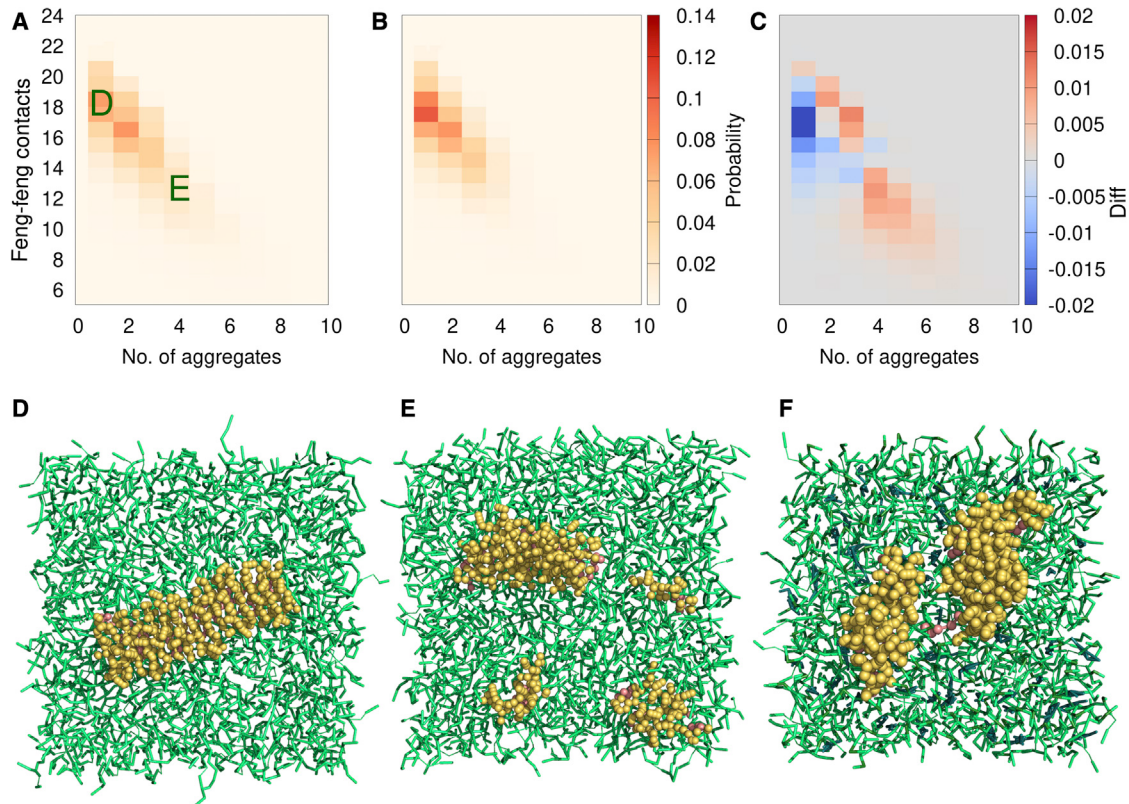


FIGURE 4 Probability of number of feng-feng contacts and number of aggregates in (A) POPC and (B) POPC:CHOL. (C) is obtained by subtracting the probabilities of (B) from (A) ($\text{POPC} - \text{POPC:CHOL}$). Example structures from different parts of the probability distribution are shown in (D)–(F); their locations on the 2D projection are indicated as green letters superposed onto (A) and (B). The molecular structures show the view from top of the membrane bilayer, with the fengycin peptide rings in yellow, the fengycin tails in salmon, POPC in lime green, and cholesterol in blue-green. To see this figure in color, go online.

Sur and Grossfield

the presence of cholesterol. This suggests that fengycin aggregation propensities might be subtly impacted by cholesterol, which in turn might have accounted for the reduced liposome leakage observed by Fiedler and Heerklotz (28).

Fengycin does not specifically pack with cholesterol or phospholipids

Our previous all-atom simulations suggested that fengycin aggregation was in part due to lack of favorable interactions with lipids, as opposed to strong specific attraction between the fengycins themselves. Here, we extend that analysis to check for preferential localization of fengycin with POPC and cholesterol. Specifically, we plotted the lateral radial distribution function between fengycin and cholesterol or POPC, shown in Fig. 5.

Other than steric exclusion at short distances, there are no major features in either radial distribution function; if there were strong favorable interactions, one would expect to see enrichment at the contact distance, causing a peak from maybe 5–8 Å. This result is not consistent with the hypothesis proposed by Fiedler and Heerklotz (28), who suggested that specific hydrogen bonds between cholesterol and fengycin could reduce fengycin aggregation. These results are similar to our previous all-atom simulations, which also failed to show specific enrichment between POPC and fengycin (32).

Another common hypothesis for the action of antimicrobial peptides is demixing of the membrane. To check for this, we computed radial distribution functions for cholesterol-cholesterol, POPC-POPC, and POPC-cholesterol in the presence and absence of fengycin; no enhanced sampling was needed to acquire good data for the pure membranes, so conventional molecular dynamics simulations were used (see Table 1).

Fig. 6 shows that the cholesterol-cholesterol and POPC-POPC distributions are not significantly perturbed by fengycin; the curves with and without fengycin superimpose almost exactly. However, there are some differences in the

POPC-cholesterol distribution within the first solvation shell. The presence of fengycin reduces the main contact peak—presumably because those contacts are replaced by fengycin—although there is a small increase in the population at very short distances. However, there is no perturbation beyond about 10 Å and thus no effect on overall lateral structure of the membrane. Thus, we can conclude that fengycin is not preferentially interacting with cholesterol or POPC and there is no demixing of the lipids in the presence of cholesterol that will affect fengycin aggregation.

Does cholesterol alter local lipid environment around fengycins?

Since fengycin does not change the lateral organization of the membrane, we now consider an alternative hypothesis, that fengycin alters the local structure of the bilayer, specifically the lipid packing, in a cholesterol-dependent manner. To test this, we examine the two-dimensional probability distribution for fengycin-fengycin and fengycin-lipid contacts, shown in Fig. 7; Fig. 7, A and B shows the results for the POPC and POPC:cholesterol bilayers, respectively, whereas Fig. 7C shows the difference map.

Although the two distributions are qualitatively similar, the POPC:CHOL distribution is broader, with the distribution shifted toward more fengycin-fengycin contacts and fewer fengycin-lipid contacts; this is most easily seen in Fig. 7C. This supports the argument mentioned above that cholesterol slightly increases fengycin aggregation by reducing the favorability of fengycin-lipid interactions.

Cholesterol limits fengycin's disordering effects

Our other alternate hypothesis was that fengycin acts in a cholesterol-dependent manner by locally deforming or disordered the membrane. We test this by quantifying the lipid chain packing surrounding the fengycin aggregates using the molecular order parameter, a measure of whole-chain

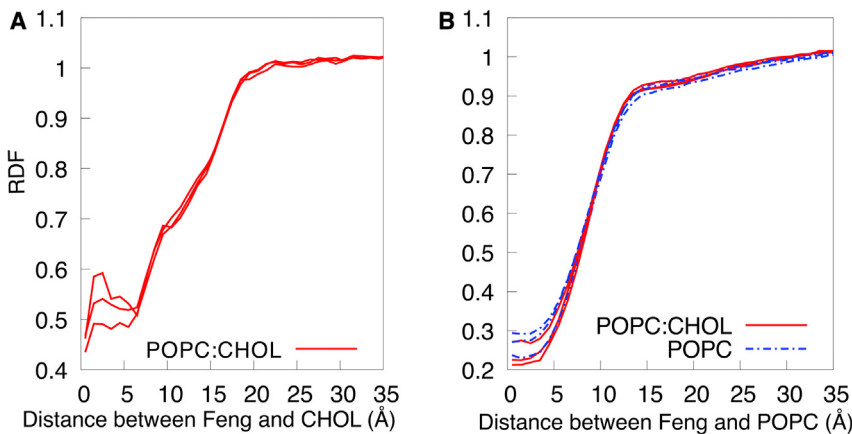


FIGURE 5 Lateral RDF between (A) cholesterol and fengycins and (B) POPC and fengycins. Results from each weighted ensemble run are shown as individual curves. To see this figure in color, go online.

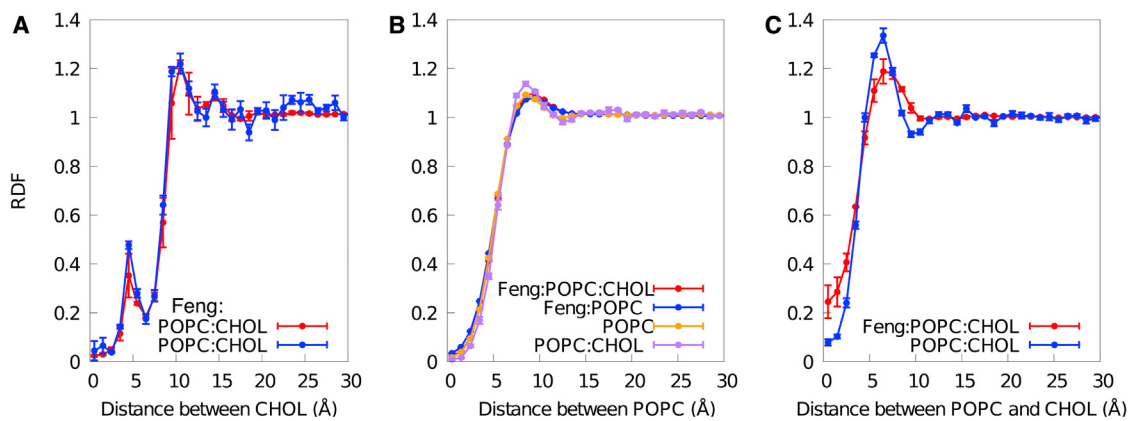


FIGURE 6 Lateral RDF between (A) cholesterols, (B) POPCs, and (C) POPC and cholesterol. All the lipid-lipid RDFs are compared with their analogous value with no fengycins present. To see this figure in color, go online.

tilt (see section [molecular order parameters](#) for details). [Fig. 8 A](#) shows the molecular order parameter for POPC palmitoyl chains calculated as a function of lateral distance to the nearest fengycin. For comparison purposes, we also show the average result for the membranes with no fengycins added. The results show that the chain order is reduced at all distances in both systems, but unsurprisingly, the effect is strongest close to the fengycin.

In [Fig. 8 B](#), we have subtracted the bulk values (the dotted lines) from the distance-dependent curves to simplify the process of quantifying difference in fengycin's effect on the two systems, setting aside the fact that cholesterol already makes membranes thicker and more ordered. The curves computed for the POPC:cholesterol system are more negative at all distance ranges, which means fengycin reduced the chain order of those membrane lipids more than it did for the neat POPC membranes, although overall, the cholesterol-containing membranes are still more ordered.

To better understand this somewhat surprising result, we broaden this comparison to determine how the molecular order parameter simultaneously varies with distance and the aggregation state of the fengycin, shown in [Fig. 9](#). As expected, the same basic trend is observed: more fengycin-fengycin contacts implies more aggregation, which leads

to lower molecular order parameters, particularly for those lipids close to the fengycin. However, when we examine the variation with distance, it is clear that, for any degree of aggregation, the reduced order parameters die off over shorter distances in cholesterol-containing membranes than in POPC systems. This suggests a different mechanism for protection by cholesterol: cholesterol renders the membrane resistant toward the local disordering effects both because it increases the baseline order and because it makes fengycin's effects short ranged.

Fengycin bends the membrane

The previous coarse-grained simulations from Horn et al. (31) suggested that fengycin aggregates systematically bend the membrane when bound to one leaflet. This suggests a new question: does cholesterol impact the asymmetry stress induced by fengycin binding to one leaflet? Visual inspection of the present simulations suggested the behavior is similar to what was observed by Horn et al. To quantify this, we calculated the height of phospholipid heads—the distance to the center of the bilayer—with respect to the distance to the nearest fengycin, as discussed in the section [Z-position of phosphate heads](#).

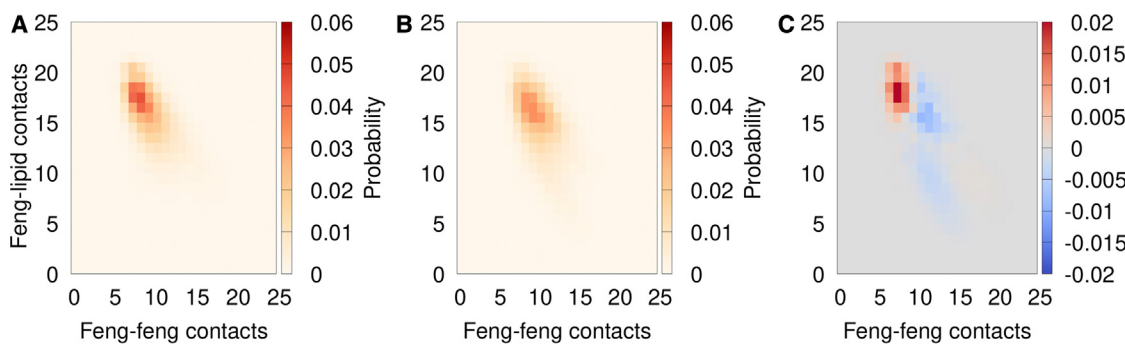


FIGURE 7 Probability of number of feng-feng contacts and number of feng-lipid contacts. (A) POPC, (B) POPC:CHOL, and (C) POPC-POPC:CHOL are shown. We used [Eqs. 1](#) and [2](#) to calculate the different contacts. To see this figure in color, go online.

Sur and Grossfield

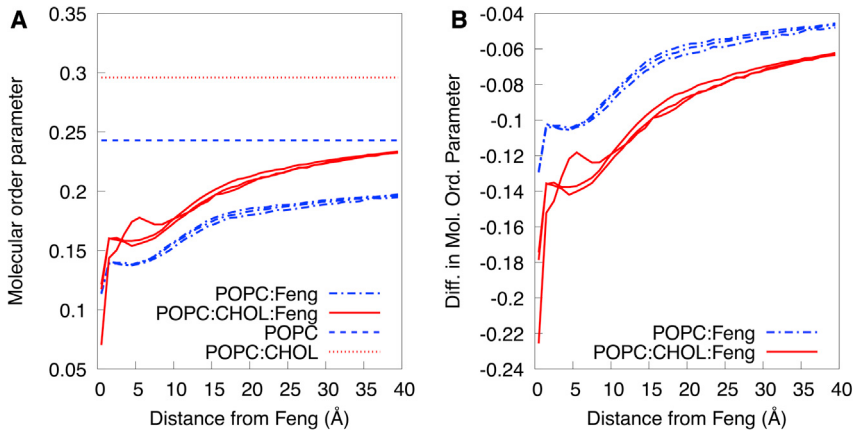


FIGURE 8 Molecular order parameters as a function of distance from nearest fengycin. (A) Average molecular order parameters as a function of distance from fengycins are shown. (B) Difference between the distance-dependent molecular order parameter and the equivalent neat lipid system is shown. Each curve shows the average in each for a single weighted ensemble replicate. To see this figure in color, go online.

To simplify comparison between membranes with different thicknesses, we subtracted the average height of the phosphates from that leaflet in the neat simulations. The results are shown in Fig. 10. Both compositions exhibit positive curvature; both leaflets are deflected in the +Z direction. Interestingly, the upper leaflets are distorted similarly, regardless of the composition of the surrounding membrane. By contrast, the lower leaflets' response varies with cholesterol: the dynamic range for the lower leaflet's deflection is 4 Å for POPC vs. 2.5 Å for the POPC:cholesterol mixture.

The positive value for the lower leaflet indicates that the lower leaflet is pushed toward the membrane center. Since the deflection of the lower leaflet is larger than that for the upper leaflet, we conclude that the fengycin aggregates simultaneously bend and thin the membrane. The upper leaflet bending is similar with and without cholesterol, but

the lower leaflet deflection is reduced by cholesterol. This leads us to conclude again that cholesterol reduces the ability of fengycin to thin the membrane. It is worth noting that the overall amplitude of bending is most likely reduced by finite-size effects, since the bilayer contains only 186 lipids per leaflet.

DISCUSSION

The primary goal of the present work has been to quantitate the aggregation of fengycin in membranes and determine the role played by cholesterol in modulating that aggregation. This required developing a novel protocol to study the thermodynamics of peptide aggregation; previous simulation work focused only on the presence or absence of aggregates (essentially focusing on the sign of the ΔG). Here, we presented an enhanced sampling approach based on the

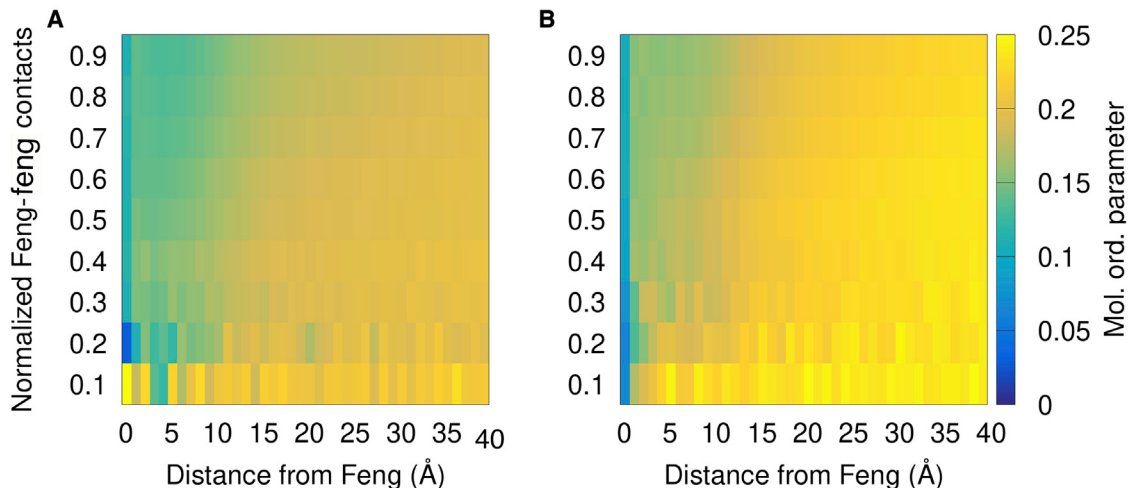


FIGURE 9 Average molecular order parameter for the palmitoyl chains as a function of distance from fengycin and fraction of fengycin-fengycin contacts. (A) POPC and (B) POPC:CHOL are shown. The x axis is the lateral distance to the nearest fengycins, and the y axis is the fraction of the fengycin-fengycin contacts obtained by dividing the fengycin-fengycin contact with the highest measured fengycin-fengycin contacts. The color range indicates the molecular order parameter for the palmitoyl chains of POPC. To see this figure in color, go online.

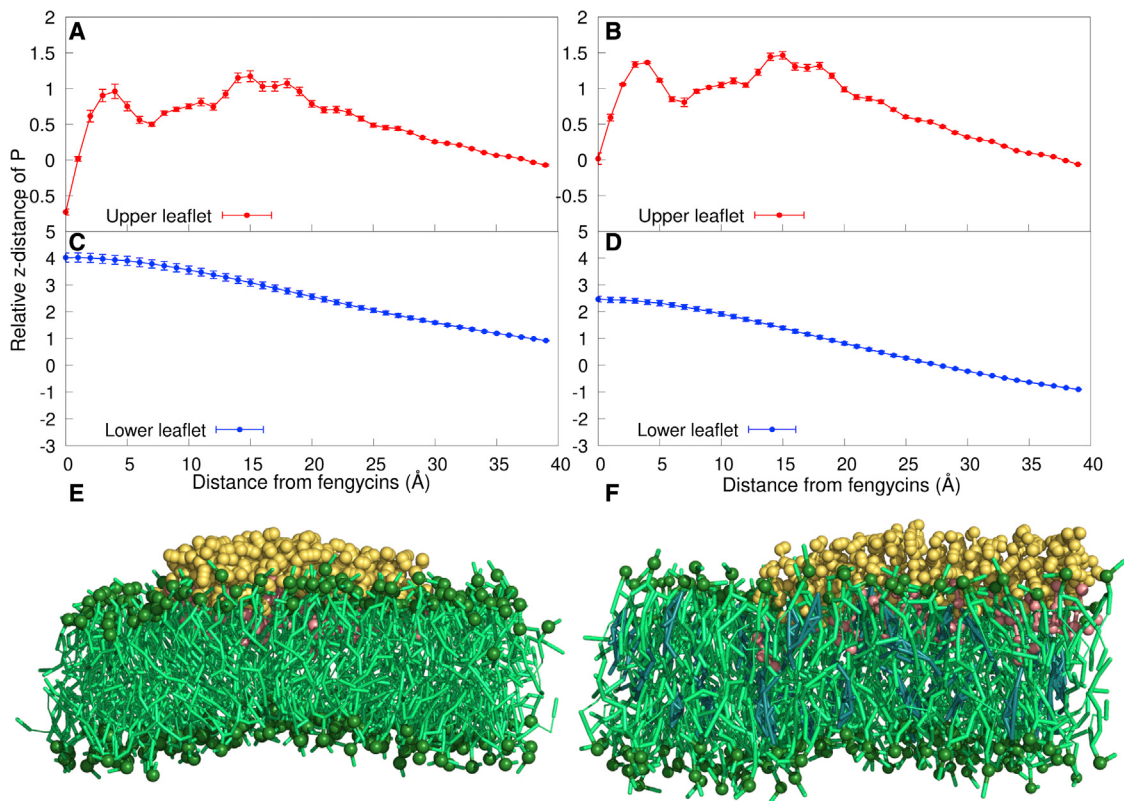


FIGURE 10 Relative Z distances of phosphates for POPC (*A* and *C*) and POPC:CHOL (*B* and *D*) as a function of distance from fengycin. The *x* axis is the distance of phospholipid from fengycin, whereas *y* axis denotes the height of phosphate moiety in the phospholipids after taking into account the thickness of the membrane. Each weighted ensemble run is considered as a single measurement, and standard error is calculated using this assumption. (*E*) and (*F*) show images of fengycin aggregates in POPC and POPC:CHOL, respectively, viewed along the plane of the membrane. The fengycin peptide head groups are yellow, the fengycin tails are salmon, POPC is shown in lime green with the phosphate beads a bit darker, and cholesterol is blue-green in color. To see this figure in color, go online.

WE algorithm, which allowed us to detect subtle shifts in the aggregation behavior of fengycin in membranes with and without cholesterol.

As we were testing and developing a new method, we chose to perform the simulations using coarse-grained models, specifically the MARTINI coarse-grained force field, as opposed to fully atomistic models. This decision comes with certain trade-offs. On one hand, the coarse-grained models are computationally efficient, which was crucial to the success of the project. Lateral reorganization of the membrane is intrinsically a slow process and even with enhanced sampling remains computationally expensive. At the same time, it was essential to run multiple independent calculations of each system, as this is the most reliable way to assess statistical uncertainties.

On the other hand, coarse-grained models by definition have less resolution than their atomistic counterparts, and that loss of resolution can at times affect both the research strategy and the results. For example, where mammalian membranes generally contain cholesterol, many fungal membranes contain ergosterol. The present work focused on the effects of the presence or absence of cholesterol,

but going forward with ergosterol is the next logical step, especially given the recent work showing that ergosterol also modulates fengycin function (48,49). However, in the context of the MARTINI model, cholesterol and ergosterol are very similar, so much so that distinguishing their effects appeared unlikely to succeed. We confirmed this by running coarse-grained simulations with ergosterol; the membrane properties are very similar to those for equivalent cholesterol-containing bilayers (see Table S1 and Fig. S1) and found that their membrane bulk properties, like area per lipid and molecular order parameters, are quite similar to cholesterol-containing bilayers. Thus, we suspect that comparing the effects of cholesterol and ergosterol will require more expensive fully atomistic simulations.

The other major issue is the known tendency of the MARTINI v.2.0 model to over-stabilize protein-protein interactions (29,50,51). We believe this manifests in the present work by causing the peptide aggregates to be more ordered than they were in our previous atomistic simulations; (32) forming stacked-disk aggregates maximizes protein-protein contact for cyclic peptides, such as fengycin. The recently released MARTINI v.3.0 addresses this

Sur and Grossfield

specific issue, but since it does not contain parameters for cholesterol, it cannot be used for the present problem (52).

However, our earlier work showed that this effect is not overwhelming, in that some membrane compositions still did not lead to stable aggregates (53). The main difference is that, in those membranes, there were favorable electrostatic lipid-peptide interactions that effectively competed with peptide-peptide packing, where in the present work, we see no evidence for specific interactions between fengycin and either the POPC head groups or cholesterol.

We chose to perform our simulations with fengycins bound to only one bilayer leaflet, to mimic the biologically relevant case where fengycin micelles encounter fungal cells and bind to the outer leaflet of their membranes. Whereas simulating the equilibrium situation, with fengycins bound to both leaflets, would also be valid, we chose the asymmetric case because that very asymmetry may play a role in function. Wimley and co-workers have shown that some cell-penetrating peptides induce permeabilization that dissipates on the timescale of minutes (54,55). They explain this phenomenon by positing that the leakage occurs with the peptides bound only to the outer leaflet of the vesicles; as the peptides gradually equilibrate to the other leaflet, the asymmetry stress is relieved and leakage ceases. Although we do observe some cholesterol flipping between leaflets, our simulations are far too short to observe the equivalent process for fengycins.

Lipopeptides, such as fengycin, are unlikely to exist as monomers in solution; rather, one would expect to see the formation of micelles that can bury the acyl chain while leaving the relatively polar peptide portion exposed to water. Previous work from our group on a different family of lipopeptides showed that blue varying kinetics of binding from a micellar state provided an alternative explanation for membrane selectivity (56). These were exceptionally challenging calculations, but it would be interesting going forward to determine whether analogous phenomena are relevant here and, in particular, whether cholesterol and/or ergosterol modify the binding kinetics of fengycin micelles.

CONCLUSIONS

Fengycins are antifungal lipopeptides that permeabilize fungal membranes while leaving the bacterial species synthesizing it unharmed and causing minimal damage to mammalian cells. The present work is a step toward understanding their mechanism, which characterizes the propensity to aggregate and how that aggregation is modulated by cholesterol. We conclude that cholesterol subtly shifts the aggregation propensity, and more significantly, the presence of cholesterol reduces the range over which fengycin perturbs the membrane. These actions are not the result of direct specific interactions between fengycin and cholesterol but rather reflect the balance of interactions between all membrane constituents.

SUPPORTING MATERIAL

Supporting material can be found online at <https://doi.org/10.1016/j.bpj.2022.04.006>.

AUTHOR CONTRIBUTIONS

S.S. performed the simulations and wrote the manuscript. A.G. conceived the project, guided the research, and edited the manuscript.

ACKNOWLEDGMENTS

We thank the Department of Biochemistry and Biophysics at the University of Rochester Medical Center for their support throughout this project. We also appreciate the computing resources provided by Center for Integrated Research Computing at the University of Rochester. The other members of our lab, Dr. Tod D. Romo and Dr. Leslie Salas-Estrada, provided critical insights throughout the project. We thank Dr. Heiko Heerklotz and the reviewers for their suggestions to improve the manuscript.

DECLARATION OF INTERESTS

A.G. is a consultant for Moderna, Inc. and Atelerix Life Sciences and holds equity in Atelerix Life Sciences. S.S. is currently a scientist at Moderna, Inc. and holds equity in Moderna, Inc.

REFERENCES

1. Worldometer Population. <https://www.worldometers.info/world-population/>.
2. Mullan, B., and J. Haqq-Misra. 2019. Population growth, energy use, and the implications for the search for extraterrestrial intelligence. *Futures*. 106:4–17. <https://doi.org/10.1016/j.futures.2018.06.009>.
3. Moore, D., G. D. Robson, and A. P. Trinci. 2011. 21st century guidebook to fungi OUTLINE. In *Outline Classification of Fungi*. Cambridge University Press.
4. Gray, K. C., D. S. Palacios, ..., M. D. Burke. 2012. Amphotericin primarily kills yeast by simply binding ergosterol. *Proc. Natl. Acad. Sci. U S A*. 109:2234–2239. <https://doi.org/10.1073/pnas.1117280109>.
5. Hammond, S. 1977. Biological activity of polyene antibiotics. *Prog. Med. Chem.* 14:Elsevier.
6. Silva, L., A. Coutinho, ..., M. Prieto. 2006. Competitive binding of cholesterol and ergosterol to the polyene antibiotic nystatin. A fluorescence study. *Biophysical J.* 90:3625–3631. <https://doi.org/10.1529/biophysj.105.075408>.
7. Avis, T. 2007. Antifungal compounds that target fungal membranes: applications in plant disease control. *Can. J. Plant Pathol.* 29:323–329. <https://doi.org/10.1080/07060660709507478>.
8. Ongena, M., P. Jacques, ..., P. Thonart. 2005. Involvement of fengycin-type lipopeptides in the multifaceted biocontrol potential of *Bacillus subtilis*. *Appl. Microbiol. Biotechnol.* 69:29–38. <https://doi.org/10.1007/s00253-005-1940-3>.
9. Ongena, M., and P. Jacques. 2008. *Bacillus* lipopeptides: versatile weapons for plant disease biocontrol. *Trends Microbiol.* 16:115–125. <https://doi.org/10.1016/j.tim.2007.12.009>.
10. Li, X. Y., Z. C. Mao, ..., C. L. Long. 2013. Diversity and active mechanism of fengycin-type cyclopeptides from *Bacillus subtilis* XF-1 against Plasmodiophora brassicae. *J. Microbiol. Biotechnol.* 23:313–321. <https://doi.org/10.4014/jmb.1208.08065>.
11. Hu, L. B., Z. Q. Shi, ..., Z. M. Yang. 2007. Fengycin antibiotics isolated from B-FS01 culture inhibit the growth of *Fusarium moniliforme*

Effects of cholesterol on fengycin

- Sheldon ATCC 38932. *FEMS Microbiol. Lett.* 272:91–98. <https://doi.org/10.1111/j.1574-6968.2007.00743.x>.
12. Chan, Y.-K., M. E. Savard, ..., C. Seguin. 2009. Identification of lipopeptide antibiotics of a *Bacillus subtilis* isolate and their control of *Fusarium graminearum* diseases in maize and wheat. *BioControl*. 54:567–574. <https://doi.org/10.1007/s10526-008-9201-x>.
 13. Romero, D., A. de Vicente, ..., A. Pérez-García. 2007. Effect of lipopeptides of antagonistic strains of *Bacillus subtilis* on the morphology and ultrastructure of the cucurbit fungal pathogen *Podosphaera fusca*. *J. Appl. Microbiol.* 103:969–976. <https://doi.org/10.1111/j.1365-2672.2007.03323.x>.
 14. Touré, Y., M. Ongena, ..., P. Thonart. 2004. Role of lipopeptides produced by *Bacillus subtilis* GA1 in the reduction of grey mould disease caused by *Botrytis cinerea* on apple. *J. Appl. Microbiol.* 96:1151–1160. <https://doi.org/10.1111/j.1365-2672.2004.02252.x>.
 15. Tao, Y., X.-M. Bie, ..., Z.-X. Lu. 2011. Antifungal activity and mechanism of fengycin in the presence and absence of commercial surfactin against *Rhizopus stolonifer*. *J. Microbiol.* 49:146–150. <https://doi.org/10.1007/s12275-011-0171-9>.
 16. Walker, R., A. A. Powell, and B. Seddon. 1998. *Bacillus* isolates from the spermosphere of peas and dwarf French beans with antifungal activity against *Botrytis cinerea* and *Pythium* species. *J. Appl. Microbiol.* 84:791–801. <https://doi.org/10.1046/j.1365-2672.1998.00411.x>.
 17. Chen, H., X. Xiao, ..., Z. Yu. 2008. Antagonistic effects of volatiles generated by *Bacillus subtilis* on spore germination and hyphal growth of the plant pathogen, *Botrytis cinerea*. *Biotechnol. Lett.* 30:919–923. <https://doi.org/10.1007/s10529-007-9626-9>.
 18. Walker, R., C. Ferguson, ..., E. Allan. 2002. The symbiosis of *Bacillus subtilis* L-forms with Chinese cabbage seedlings inhibits conidial germination of *Botrytis cinerea*. *Lett. Appl. Microbiol.* 34:42–45. <https://doi.org/10.1046/j.1472-765x.2002.01037.x>.
 19. Zhou, X., Z. Lu, ..., X. Bie. 2011. Antagonistic action of *Bacillus subtilis* strain fmbj on the postharvest pathogen *rhizopus stolonifer*. *J. Food Sci.* 76:M254–M259. <https://doi.org/10.1111/j.1750-3841.2011.02160.x>.
 20. Vanittanakom, N., W. Loeffler, ..., G. Jung. 1986. Fengycin—a novel antifungal lipopeptide antibiotic produced by *Bacillus subtilis* F-29-3. *J. Antibiot.* 39:888–901. <https://doi.org/10.7164/antibiotics.39.888>.
 21. Schneider, J., K. Taraz, ..., P. Jacques. 1999. The structure of two fengycins from *Bacillus subtilis* S499. *Zeitschrift für Naturforschung C*. 54:859–866. <https://doi.org/10.1515/znc-1999-1102>.
 22. Eeman, M., M. Deleu, ..., Y. F. Dufrêne. 2005. Nanoscale properties of mixed fengycin/ceramide monolayers explored using atomic force microscopy. *Langmuir*. 21:2505–2511. <https://doi.org/10.1021/la0475775>.
 23. Eeman, M., G. Francius, ..., M. Deleu. 2009. Effect of cholesterol and fatty acids on the molecular interactions of fengycin with Stratum corneum mimicking lipid monolayers. *Langmuir*. 25:3029–3039. <https://doi.org/10.1021/la803439n>.
 24. Eeman, M., G. Olofsson, ..., M. Deleu. 2014. Interaction of fengycin with stratum corneum mimicking model membranes: a calorimetry study. *Colloids Surf. B Biointerfaces*. 121:27–35. <https://doi.org/10.1016/j.colsurfb.2014.05.019>.
 25. Heerklotz, H. 2008. Interactions of surfactants with lipid membranes. *Q. Rev. Biophys.* 41:205–264. <https://doi.org/10.1017/s0033583508004721>.
 26. Heerklotz, H. 2001. Membrane stress and permeabilization induced by asymmetric incorporation of compounds. *Biophysical J.* 81:184–195. [https://doi.org/10.1016/s0006-3495\(01\)75690-1](https://doi.org/10.1016/s0006-3495(01)75690-1).
 27. Patel, H., C. Tscheka, ..., H. Heerklotz. 2011. All-or-none membrane permeabilization by fengycin-type lipopeptides from *Bacillus subtilis* {QST713}. *Biochim. Biophys. Acta Biomembr.* 1808:2000–2008.
 28. Fiedler, S., and H. Heerklotz. 2015. Vesicle leakage reflects the target selectivity of antimicrobial lipopeptides from *Bacillus subtilis*. *Biophysical J.* 109:2079–2089. <https://doi.org/10.1016/j.bpj.2015.09.021>.
 29. de Jong, D. H., G. Singh, ..., S. J. Marrink. 2013. Improved parameters for the martini coarse-grained protein force field. *J. Chem. Theor. Comput.* 9:687–697. <https://doi.org/10.1021/ct300646g>.
 30. Zuckerman, D. M., and L. T. Chong. 2017. Weighted ensemble simulation: review of methodology, applications, and software. *Annu. Rev. Biophys.* 46:43–57. <https://doi.org/10.1146/annurev-biophys-070816-033834>.
 31. Horn, J. N., T. D. Romo, and A. Grossfield. 2013. Simulating the mechanism of antimicrobial lipopeptides with all-atom molecular dynamics. *Biochemistry*. 52:5604–5610. <https://doi.org/10.1021/bi400773q>.
 32. Sur, S., T. D. Romo, and A. Grossfield. 2018. Selectivity and mechanism of fengycin, an antimicrobial lipopeptide, from molecular dynamics. *J. Phys. Chem. B.* 122:2219–2226. <https://doi.org/10.1021/acs.jpcb.7b11889>.
 33. Marrink, S. J., H. J. Risselada, ..., A. H. de Vries. 2007. The MARTINI force field: coarse grained model for biomolecular simulations. *J. Phys. Chem. B.* 111:7812–7824. <https://doi.org/10.1021/jp071097f>.
 34. Monticelli, L., S. K. Kandasamy, ..., S.-J. Marrink. 2008. The MARTINI coarse-grained force field: extension to proteins. *J. Chem. Theor. Comput.* 4:819–834. <https://doi.org/10.1021/ct700324x>.
 35. Melo, M. N., H. I. Ingólfsson, and S. J. Marrink. 2015. Parameters for Martini sterols and hopanoids based on a virtual-site description. *J. Chem. Phys.* 143:243152. <https://doi.org/10.1063/1.4937783>.
 36. Wassenaar, T. A., H. I. Ingólfsson, ..., S. J. Marrink. 2015. Computational lipidomics with insane: a versatile tool for generating custom membranes for molecular simulations. *J. Chem. Theor. Comput.* 11:2144–2155. <https://doi.org/10.1021/acs.jctc.5b00209>.
 37. Abraham, M. J., T. Murtola, ..., E. Lindahl. 2015. GROMACS: high performance molecular simulations through multi-level parallelism from laptops to supercomputers. *SoftwareX*. 1–2:19–25. <https://doi.org/10.1016/j.softx.2015.06.001>.
 38. Parrinello, M., and A. Rahman. 1981. Polymorphic transitions in single crystals: a new molecular dynamics method. *J. Appl. Phys.* 52:7182–7190. <https://doi.org/10.1063/1.328693>.
 39. Bussi, G., D. Donadio, and M. Parrinello. 2007. Canonical sampling through velocity rescaling. *J. Chem. Phys.* 126:014101. <https://doi.org/10.1063/1.2408420>.
 40. Barker, J., and R. Watts. 1973. Monte Carlo studies of the dielectric properties of water-like models. *Mol. Phys.* 26:789–792. <https://doi.org/10.1080/0026897300102101>.
 41. Zwier, M. C., J. L. Adelman, ..., L. T. Chong. 2015. WESTPA: an interoperable, highly scalable software package for weighted ensemble simulation and analysis. *J. Chem. Theor. Comput.* 11:800–809. <https://doi.org/10.1021/ct5010615>.
 42. Zwier, M. C., J. L. Adelman, ..., and L. T. Chong. WESTPA 1.0. <https://github.com/westpa/westpa>.
 43. Romo, T., and A. Grossfield. 2014. Unknown unknowns: the challenge of systematic and statistical error in molecular dynamics simulations. *Biophysical J.* 106:1553–1554. <https://doi.org/10.1016/j.bpj.2014.03.007>.
 44. Romo, T. D., and A. Grossfield. 2009. LOOS: an extensible platform for the structural analysis of simulations. *Conf. Proc. IEEE Eng. Med. Biol. Soc.* 2009:2332–2335. <https://doi.org/10.1109/emb.2009.5330565>.
 45. Romo, T. D., and A. Grossfield. LOOS: A Lightweight Object-Oriented Structure Analysis Library. <http://grossfieldlab.github.io/loos/>.
 46. Seelig, J. 1977. Deuterium magnetic resonance: theory and application to lipid membranes. *Q. Rev. Biophys.* 10:353–418. <https://doi.org/10.1017/s0033583500002948>.
 47. Javanainen, M., H. Martinez-Seara, and I. Vattulainen. 2017. Excessive aggregation of membrane proteins in the Martini model. *PLoS One*. 12: e0187936–20. <https://doi.org/10.1371/journal.pone.0187936>.
 48. Mantil, E., T. Crippin, and T. J. Avis. 2019. Supported lipid bilayers using extracted microbial lipids: domain redistribution in the presence of fengycin. *Colloids Surf. B Biointerfaces*. 178:94–102. <https://doi.org/10.1016/j.colsurfb.2019.02.050>.

Sur and Grossfield

49. Mantil, E., T. Crippin, and T. J. Avis. 2019. Domain redistribution within ergosterol-containing model membranes in the presence of the antimicrobial compound fengycin. *Biochim. Biophys. Acta Biomembr.* 1861:738–747. <https://doi.org/10.1016/j.bbamem.2019.01.003>.
50. Stark, A. C., C. T. Andrews, and A. H. Elcock. 2013. Toward optimized potential functions for protein–protein interactions in aqueous solutions: osmotic second virial coefficient calculations using the MARTINI coarse-grained force field. *J. Chem. Theor. Comput.* 9:4176–4185. <https://doi.org/10.1021/ct400008p>.
51. Nishizawa, M., and K. Nishizawa. 2014. Potential of mean force analysis of the self-association of leucine-rich transmembrane α -helices: difference between atomistic and coarse-grained simulations. *J. Chem. Phys.* 141:075101. <https://doi.org/10.1063/1.4891932>.
52. Souza, P. C. T., R. Alessandri, and S. J. Marrink. 2021. Martini 3: a general purpose force field for coarse-grained molecular dynamics. *Nat. Methods.* 18:382–388. <https://doi.org/10.1038/s41592-021-01098-3>.
53. Horn, J. N., A. Cravens, and A. Grossfield. 2013. Interactions between fengycin and model bilayers quantified by coarse-grained molecular dynamics. *Biophysical J.* 105:1612–1623. <https://doi.org/10.1016/j.bpj.2013.08.034>.
54. Krauson, A. J., J. He, and W. C. Wimley. 2012. Determining the mechanism of membrane permeabilizing peptides: identification of potent, equilibrium pore-formers. *Biochim. Biophys. Acta Biomembr.* 1818:1625–1632. <https://doi.org/10.1016/j.bbamem.2012.02.009>.
55. Wimley, W. C. 2015. Determining the Effects of Membrane-Interacting Peptides on Membrane Integrity. Springer, New York, NY, pp. 89–106.
56. Lin, D., and A. Grossfield. 2015. Thermodynamics of micelle formation and membrane fusion modulate antimicrobial lipopeptide activity. *Biophys. J.* 109:750–759. <https://doi.org/10.1016/j.bpj.2015.07.011>.